Atomistic modeling of ion channeling in Si with point defects: The role of lattice relaxation

Simone Balboni
Dipartimento di Fisica dell' Università di Bologna, Viale Berti Pichat 6/2, I–40126 Bologna, Italy

Eros Albertazzi, Marco Bianconi, and Giorgio Lulli*
Consiglio Nazionale delle Ricerche - Istituto per la Microelettronica e i Microsistemi, Sezione di Bologna, Via P. Gobetti 101, I–40129 Bologna, Italy

(Received 16 February 2002; published 8 July 2002)

We report the results of the simulation of ion-channeling spectra in a disordered silicon crystal, where lattice relaxation in the neighborhood of point defects, calculated by the application of empirical potentials, is taken into account. We show that, in general, the backscattering yield increases when the perfectly symmetrical configurations of point defects in the unperturbed lattice are allowed to relax. The yield enhancement depends on the potential used, the point defect type, and the beam-lattice alignment condition. A quantitative correlation between the microscopic disorder and the macroscopic yield measured by ion channeling, has been determined under the condition of a low concentration of weakly interacting point defects. The practical consequences of introducing relaxation in the interpretation of Rutherford backscattering-channeling spectra are pointed out and discussed. One important result is that if relaxation effects are neglected (as in damage models used so far), the amount of defects extracted from channeling analysis may be appreciably overestimated. The method developed here has been applied to the study of the damage distribution in the near surface of a Si sample implanted with high energy ions. In spite of the simplified description of damage in terms of point defects, our preliminary results show that taking into account lattice relaxation in ion-channeling simulation allows simultaneous fitting of backscattering spectra collected along different axial alignment conditions. The same result cannot be achieved using the standard description based on unrelaxed defects.

DOI: 10.1103/PhysRevB.66.045202 PACS number(s): 61.85.+p, 61.72.Ji, 82.80.Yc, 61.80.Jh

I. INTRODUCTION

Due to its huge importance in microelectronic technology, crystalline silicon is still one of the materials most investigated in the field of radiation damage physics. The goal is to improve the understanding and control of the mechanisms of defect formation during irradiation with charged particles (ions, electrons), used nowadays as a standard process to modify the material properties by the introduction of either impurities or lattice defects.

The advances in atomic-scale computational techniques have recently led to relevant progress in modeling radiation damage in Si. Classical molecular dynamics (MD) using empirical interatomic potentials[1–3] has enabled the simulation of the collision cascades, generated in Si by the impact of ions at energies up to some tens of keV.[4–7] On the other hand, more computationally intensive quantum-mechanical methods have been applied to the study of smaller-scale radiation-damage problems, such as the dynamics of low-energy recoils in Si,[8,9] or of the fundamental properties of simple defects (as concerns vacancies and self interstitials see, for example, Refs. 10–19).

Theoretical models of radiation damage are not easily validated by experiments, since the interpretation of the macroscopic response of structural characterization techniques, in terms of the amount and atomic-scale configuration of defects, is not straightforward. Experimental techniques based on x-ray diffraction and diffusion, or ion channeling, are indeed sensitive to the structural disorder in irradiated crystals. However, the simplified picture of defects usually employed to interpret the measurements is often inadequate to extract information on the microstructure of damage. For example, the simple elastic theory of point defects assumes that each Frenkel pair introduces a lattice expansion of the order of an atomic volume.[21,20] If, according to this assumption, we estimate the number of defects from the lattice strain measured in an ion-implanted Si sample by double crystal x-ray diffractometry (DCXD) and compare it with the estimate obtained from Rutherford backscattering-channeling (RBS-C) using the standard two-beam model,[22] we find that the number obtained from DCXD is about two orders of magnitude smaller that the one given by RBS-C.[23,24]

Attempts to improve the microscopic interpretation of structural measurements have been recently reported for the diffuse x-ray scattering (DXS) technique.[25–27] To simulate the DXS patterns from irradiated semiconductors, the authors have assumed a microscopic model of damage in which the relaxation of lattice atoms due to the introduction of point defects is simulated through the application of empirical potentials.

Similarly to x-ray based techniques, the response of RBS-C, one of the techniques most widely used in the last decades to characterize radiation damage in crystalline targets,[28] depends on both the amount and the microscopic configuration of lattice defects. Different methods can be used to extract quantitative information from the measurements. Some are analytical,[22,29] and mainly based on Lindhard's theory of channeling,[30] others involve full simulation of ion trajectories, which is typically performed using the Monte Carlo method within the binary collision approximation (MC-BCA).[31,32] In some treatments,[29,33] disordered atoms are put at a certain distance from the atomic strings or planes parallel to the incident beam direction. Such a dis-

placement distance, extracted as a fitting parameter, can give some hints about the configuration of defects.[33] In our previous works based on full MC-BCA simulation,[34,35] we adopted the simple description of defects as atoms displaced at random around their original lattice site. This method shares with most approaches used so far the simplification that displaced atoms are surrounded by a perfect crystal. Therefore, the lattice relaxation which occurs in the neighborhood of a defect is not taken into account. Although a few attempts to speculate about this effect have been made,[33,36] to the best of our knowledge no direct simulation of ion channeling in Si-containing relaxed configurations of point defects has been reported up to this date.

In this paper we show the results of the simulation of RBS-C spectra in a Si crystal containing point defects, relaxed by the application of empirical potentials. In order to have a basis for a better understanding of defect analysis by ion channeling, we start from a relatively simple case, i.e., a crystalline sample containing a low, uniform concentration (1 at. %) of point defects, namely vacancies and self interstitials in equal numbers. Although the damage found in as irradiated Si is actually more complex, the results for this simple case give information on some fundamental aspects, such as the sensitivity of the RBS-C response under different beam-lattice alignment conditions, to the relaxation induced by different kinds of defects and to the empirical potential used to model lattice relaxation.

Finally, as a first application of the model, we report the analysis of experimental RBS-C spectra obtained from a surface layer, 1 μm thick, of a sample implanted at RT with high energy As ions, characterized by the presence of a low (a few atomic %) level of damage. Notwithstanding the approximated description of the damaged layer in terms of simple point defects, we show that the introduction of lattice relaxation allows us to reproduce simultaneously, assuming a single distribution of a specific kind of point defects (split–$\langle 110 \rangle$ interstitials, plus equal number of vacancies), the spectra obtained under different crystallographic alignments. The same multiaxial fit is not possible if we assume unrelaxed point defects in the simulation.

II. COMPUTER SIMULATION

A. Simulation of Rutherford backscattering-channeling spectra

The computer code BISIC (Binary collision simulation of ion channeling),[34,37] used to simulate RBS-C spectra, is based on the MC-BCA method and follows the full three-dimensional treatment of ion penetration in the crystal, as described in Ref. 38. Using the close encounter probability[31] and the Rutherford scattering cross section, and approximating the backscattered paths with straight trajectories, the program gives as output the yield at the detector as a function of energy, which can be directly compared with its experimental counterpart. The default procedure to describe lattice disorder in the simulation is to displace atoms at random around their original lattice site, leaving the surrounding crystal unperturbed. The method is similar to the one reported in Ref. 39 for the simulation of ion implantation in crystalline Si. The result is a pseudo-Frenkel pair, where the self interstitial and the corresponding empty site (vacancy) are separated by a distance which, according to the chosen displacement distribution, is on average about 1.44 Å. We refer to these defects as ''random.'' The method to extract damage profiles from RBS-C measurements is to vary the concentration depth profile of random defects in the simulation, until the experimental RBS-C spectrum is reproduced. It is worth reminding that this method, although more accurate, gives results which are quantitatively similar to those obtained from the standard analysis based on the ''two beams'' approximation.[34,22]

In previous works[36,40] we have pointed out some misleading results to which such a simplified picture of radiation damage may lead. For example, it is rather intuitive that if we try to extract quantitative information from the RBS-C yield neglecting lattice relaxation, we will systematically need a larger number of point defects to account for the dechanneling which is due to lattice distortion around defects themselves.

To demonstrate these qualitative considerations, and to improve the picture of lattice damage used in the simulation of RBS-C spectra, we have thus introduced atomistic structures of point defects calculated by the application of classical empirical potential, as described in the following.

B. Point defects and lattice relaxation

The size of the Si supercell required for ion-channeling simulation must be large enough to ensure a good statistical sampling of the damaged crystal and to avoid size dependent artifacts. For instance, if we use too small cells and replicate them to build the whole region crossed by the analyzing ion beam, we introduce an in-depth periodicity which leads to anomalies in the RBS-C yield. We found that a choice which prevents the occurrence of such problems, is to use a large building block containing $\sim 5\times 10^5$ atoms ($9\times 14\times 500$ lattice units), with periodic boundary conditions at the surfaces.

Vacancies are obtained by removing an atom from its lattice site. The initial position of a self interstitial is chosen among the highly symmetrical hexagonal (I_H), tetrahedral (I_T), or split-$\langle 110 \rangle$ (I_S) configurations in the unrelaxed lattice. The cell is populated at random with equal numbers of self interstitials and vacant sites. In the present work we will limit the analysis to a fixed, dilute concentration (1% atomic fraction) of vacancy-interstitial pairs. We always kept a minimum interstitial-interstitial and vacancy-vacancy distance of 6.5 Å and a minimum vacancy-interstitial distance of 7 Å. This allows us to minimize possible interactions, in particular recombination or clustering of defects during relaxation.[41]

In the following treatment we will refer to the number of point defects as the number of Wigner-Seitz cells with occupation numbers of zero (vacancies) and two (interstitials). According to this criterion, each of the configurations (I_H, I_T, I_S, and the empty site) chosen to initially populate the cell corresponds to one defect in the unrelaxed lattice.

To model the structural rearrangement due to the insertion of interstitials and vacancies, three different empirical many-body interatomic potentials for Si were used: the Stillinger-

Weber (SW),[1] the Tersoff III (TS),[2] and the environment-dependent interatomic potential (EDIP).[3] The capability of these potentials to reproduce results calculated with *ab initio* methods varies according to defect type and property. In the present work, we were interested in investigating if, and to what extent, the response of ion channeling is sensitive to the model potential used to relax defects.

We adopted a static relaxation procedure at constant volume and used periodic boundary conditions. To avoid artifacts that may arise from the perfect symmetry of the initial defect configurations and from the use of a static relaxation procedure (such as the possibility of the system to stop in a saddle-point configuration[42]), we use the method of applying small random displacements both to the initial coordinates of the supercell (before relaxation), and to the final atomic coordinates. In the latter case the perturbation is followed by a further relaxation step. The random displacements are chosen according to a Gaussian distribution, with 1D standard deviation (0.0077 nm[43]) corresponding to the thermal vibration amplitude of Si atoms at room temperature. By performing different trials for each initial and final configuration, using different random number generators for the displacements, we found that the relaxed supercells are stable, in terms of their formation energy and of the yield obtained from RBS-C simulation, with respect to the perturbation of atomic coordinates.

The relaxed configurations of self interstitials are in quite good agreement with those calculated with more exact quantum-mechanical methods, while for the vacancy we do not find a structure showing the inward relaxation of first neighbors, as foreseen in Refs. 10, 16, and 17. Indeed, both TS and EDIP potentials give outward relaxation, while for the SW potential we find a structure very close to the undistorted (ideal) vacancy. This could influence the calculated RBS-C yield. In particular, when the supercell is relaxed with the SW potential, the contribution of vacancies to the yield will be underestimated. However, since the yield enhancement due to an interstitial atom is much higher than the one induced by a vacancy, the inaccuracy in the description of the latter is expected to play a minor role.

It is worth noting that in the ideal model system that we are going to study, which is representative of a dilute distribution of point defects, the overlapping of the deformation fields is small; therefore the relative contribution to dechanneling of the strained lattice around defects is expected to be maximized.

III. RESULTS AND DISCUSSION

A. Analysis of the model system

Simulations of RBS-C spectra were performed assuming a 3 MeV He^{2+} beam, a backscattering angle of 170° and a (100) Si wafer as a target. Calculations were done for the beam aligned along three main axes, corresponding to the $\langle 100\rangle$, $\langle 110\rangle$, and $\langle 112\rangle$ lattice directions.

For the quantitative comparison of spectra, we use the minimum yield (χ_{min}). The χ_{min} is defined as the ratio of the integral of the RBS-C yield in the sample of interest to the integral of the yield in the fully disordered (amorphous) material, both calculated in the same backscattering energy interval, corresponding to a near surface layer, and leaving out the peak which originates from the first impact of ions onto the surface. According to this definition, $\chi_{min}=1$ for an amorphous target. For virgin, undamaged Si, the calculated values of χ_{min} are 0.026, 0.016, and 0.032 for $\langle 100\rangle$, $\langle 110\rangle$, and $\langle 112\rangle$ alignments, respectively.

TABLE I. Values of χ_{min} (expressed in % of random yield) given by RBS-C simulation in a Si sample containing a 1% uniform concentration of I-V pairs calculated for different self-interstitial configurations and alignment conditions, and reference values for virgin Si. The analyzing beam is 3 MeV He^{2+}. Absolute statistical errors of the simulation are 0.1 for virgin Si and 0.2 in all the other cases.

		Virgin	I_T	I_H	I_S	$I_T+I_H+I_S$
Unrelaxed	$\langle 100\rangle$	*2.6*	2.6	3.6	4.0	3.3
	$\langle 110\rangle$	*1.6*	3.3	3.8	4.6	4.5
	$\langle 112\rangle$	*3.2*	4.0	5.3	5.4	5.1
TS	$\langle 100\rangle$		3.8	3.6	5.5	4.5
	$\langle 110\rangle$		4.3	4.2	4.9	4.7
	$\langle 112\rangle$		5.6	5.5	7.1	6.2
EDIP	$\langle 100\rangle$		3.7	3.6	5.1	4.4
	$\langle 110\rangle$		4.5	4.5	5.0	4.9
	$\langle 112\rangle$		5.6	5.6	6.7	6.0
SW	$\langle 100\rangle$		4.1	5.4	6.8	5.9
	$\langle 110\rangle$		4.4	5.4	5.9	5.6
	$\langle 112\rangle$		6.0	7.3	8.3	7.8

The first three samples for RBS-C simulation were prepared by introducing self interstitials in the I_T, I_H, and split-$\langle 110\rangle$ (I_S) configurations, respectively. In each case all equivalent positions and orientations were taken into account, with equal probabilities. A fourth sample was prepared introducing a mix of I_T, I_H, and I_S, in equal amounts. Vacancies were introduced in all samples to exactly balance the number of self interstitials. In order to point out the amount of extra yield due to defect-induced strain, RBS-C spectra have been simulated both before and after relaxation. All the values of χ_{min} calculated for different alignment conditions, potentials used for the relaxation, and initial defect configurations, are reported in Table I.

As a general rule, we observe that except for the sample populated with I_H, analyzed along $\langle 100\rangle$ and relaxed with TS or EDIP potentials, the χ_{min} increases upon relaxation. The relative yield enhancement depends on the defect type, on the model potential, and on the alignment condition. The most evident example of the effect of relaxation is the I_T defect. In the unrelaxed state, I_T is invisible when observed along the $\langle 100\rangle$ direction, being completely shadowed from the lattice atomic rows. Therefore, the χ_{min} of the sample containing unrelaxed I_T defects is equal to the χ_{min} of virgin Si. The atomic movements associated with relaxation lead to a condition where the atoms have a significant projection onto the $\langle 100\rangle$ channel, which explains the large increase (about 50%) in χ_{min}, observed for all model potentials. I_S is the defect which always introduces the largest yield increase, for all orientations considered. This result, which is mainly a

consequence of the fact that two atoms instead of one are significantly displaced out of regular lattice sites, is observed for both unrelaxed and relaxed samples.

As concerns the behavior of the different potentials, we find two clear trends. The first is that the TS and EDIP potentials produce relaxed supercells whose χ_{min} values are equal within the statistical errors: from the point of view of RBS-C analysis they may therefore be considered equivalent. Second, we note that the increase of disorder upon relaxation with the SW potential is almost always larger (of an average factor 1.2–1.3) than the one obtained with either the TS or EDIP ones, independently of the alignment condition. The only exception to this behavior is the I_T defect, for which the relaxation with the SW potential produces a RBS-C yield equivalent to that given by the other two. The propensity of SW Si for the perfect tetrahedral coordination may qualitatively explain this behavior. In fact, very small atomic rearrangements are expected in the neighborhood of a self-interstitial position (I_T) which already corresponds to a preferred bonding configuration.

We explored different methods to quantitatively analyze the disorder in relaxed samples, with the purpose of establishing a correlation between a microscopic measure of damage based on the analysis of the atomic displacement distribution and the χ_{min} determined by RBS-C. It must be pointed out that the number of point defects, counted according to the Wigner-Seitz cell method, does not change upon relaxation. A criterion which also takes into account smaller perturbations in crystalline order is required. Details of this analysis are reported elsewhere.[41] The main result obtained is that if the disorder of the relaxed supercells is measured as the number of atoms which are located outside the spheres of radius 0.45 Å centered around the original lattice sites (known as Lindemann spheres), a monotonic and nearly linear correlation is found between said disorder and the χ_{min} determined for all defect-potential combinations investigated. Data are reported in Fig. 1 for the three different axial-alignment conditions, where each point represents the case of a population of single defects relaxed with one of the three potentials. The points at zero disorder relative to virgin crystal are also reported. We observe a very good linear correlation for the analysis along the $\langle 100 \rangle$ and $\langle 112 \rangle$ axes (correlation coefficients 0.986 and 0.964, respectively), while under $\langle 110 \rangle$ alignment the point relative to the virgin crystal shows appreciable deviation from the linear fitting curve (overall correlation coefficient equal to 0.877). The Lindemann radius $r_L = 0.45$ Å, which identifies a threshold to mark the highly displaced atoms mainly responsible for the macroscopic RBS-C yield, is defined as the vibration amplitude of Si atoms at their melting point, calculated with the SW potential.[44] It must be pointed out that the Lindemann sphere criterion is strongly correlated with the preexisting order of the perfect crystal. For this reason it is expected to work well in the case of low defect concentration, where the integrity of the underlying lattice is mostly preserved.

As concerns the dependence of results reported in Table I on the different alignment conditions, if we look at the ratio of χ_{min} of samples containing defects (χ_{min}^{def}) to the χ_{min} in virgin Si (χ_{min}^{v}), we observe that for both unrelaxed and relaxed defects the most sensitive orientation is the $\langle 110 \rangle$, followed by the $\langle 112 \rangle$ and the $\langle 100 \rangle$. This behavior has been reported in Fig. 2, taking as an example the sample containing a mix of point defects.

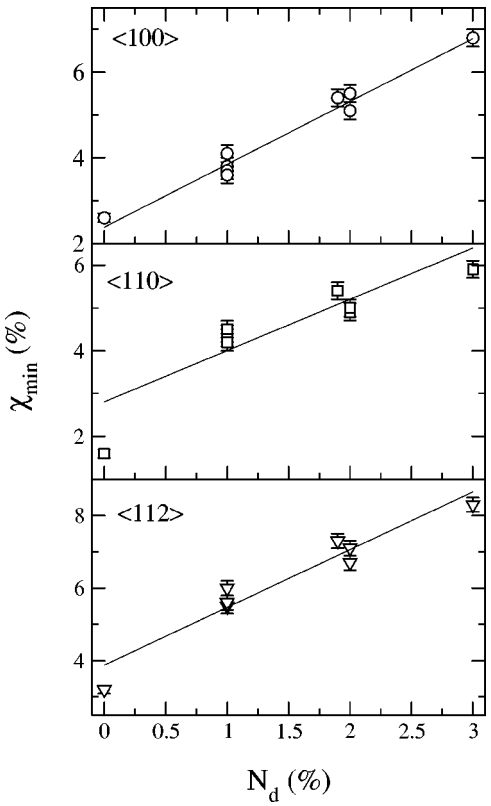

FIG. 1. RBS-C yield calculated for all single defect-potential combinations reported in Table I as a function of the number of disordered atoms (N_d) counted according to the Lindemann sphere criterion. The analysis is performed for each alignment condition investigated. The points at zero abscissa (no disorder) are relative to the virgin Si. Lines are the linear fits of data.

We have also examined how the yield increases as a function of lattice orientation, when going from unrelaxed to re-

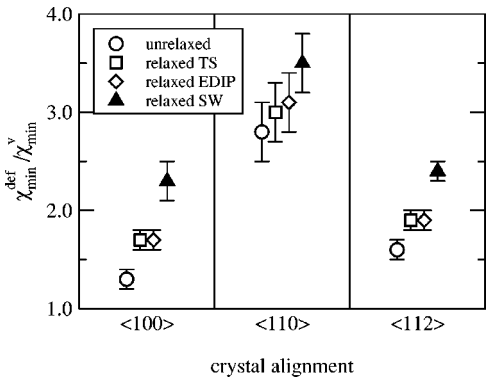

FIG. 2. Relative increase of the minimum yield with respect to virgin Si, due to introduction of a mix of 1% point defects, calculated for RBS-C along three main crystallographic directions. Values for unrelaxed samples, as well as for samples relaxed by the application of the TS, EDIP, or SW potentials, are reported.

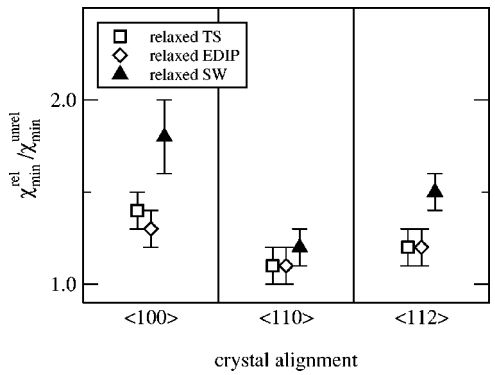

FIG. 3. Relative increase of the minimum yield for a sample containing a mix of relaxed 1% point defects, with respect to a sample containing unrelaxed defects, for the three main crystallographic directions.

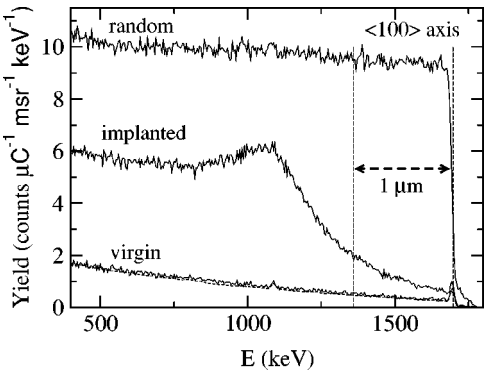

FIG. 4. Yields (absolute normalized counts) vs backscattering energy obtained by RBS-C analysis performed with 3 MeV He^{2+} ions and a backscattering angle of 170° under the ⟨100⟩ alignment. The spectrum of the implanted sample refers to irradiation with a dose of 10^{14} ions/cm^2 3 MeV As^{2+} ions. Random and virgin spectra are also reported for reference, the latter together with its simulation (dashed curve). The double dashed arrow indicates the region of the spectrum which originates from the 1 μm thick surface layer of the material.

laxed defects. In Fig. 3 we have considered the case of mixed defects as an example, and have reported the ratio of the yield of relaxed defects (χ_{min}^{rel}) to the yield of unrelaxed defects (χ_{min}^{unrel}) for the three different alignment conditions. Mixed defects show a trend similar to that already seen for I_T, the largest yield enhancement occurring for the ⟨100⟩ direction, followed by the ⟨112⟩ and the ⟨110⟩. The anisotropy in the yield enhancement upon relaxation may influence the interpretation of RBS-C spectra collected along different axial orientations. For example, it may not be possible to simultaneously fit the spectra along different axes, using unrelaxed defects. Preliminary results obtained in the near surface region of samples implanted with MeV ions, reported in the following, confirm this expectation.

B. Analysis of an ion implanted sample: Preliminary results

Here we consider a Si sample implanted at nominal room temperature with 10^{14} cm^{-2} 3 MeV As ions. We have limited the analysis to a surface layer 1 μm thick, where the damage level is low, and the approximation of dilute defects is better fullfilled. The (100) Si sample has been analyzed along the three crystallographic alignments ⟨100⟩, ⟨110⟩ and ⟨112⟩ with a 3 MeV He^{2+} beam, and a backscattering angle of 170°. More details on the experimental setup can be found in Ref. 37. The spectra measured under ⟨100⟩ alignment are reported in Fig. 4. We have tried to model the 1-μm-thick surface layer of the damaged crystal, following the procedure outlined in the previous sections, i.e., by using only simple point defects. To this purpose, a supercell with a size of $5\times5\times1900$ lattice units along ⟨100⟩, ⟨010⟩, and ⟨001⟩ crystallographic axes, respectively, was generated, corresponding to $\approx$30 Å$\times$30 Å$\times$1 μm and containing about 4×10^5 atoms. Since in the literature there is agreement about the fact that I_S is the most stable interstitial configuration in Si, we decided to start the investigation using I_S point defects, plus an equal number of vacancies, to simulate the damage. For simplicity, we have assumed a defect distributions function linearly varying with depth. In agreement with the simulation strategy depicted above, we have always kept the distance between defects at the largest values compatible with their maximum concentration.

First of all we have determined the defect distribution which reproduces the ⟨100⟩ RBS-C spectrum for three different cases: unrelaxed supercells, supercells relaxed with the TS potential, and supercells relaxed with the SW potential. For comparison, we have also reported the profile calculated by the random defect model,[34] as outlined in Sec. II A. The resulting damage profiles are reported in Fig. 5. The observed differences are easily explained by the results already reported in the analysis of the model system. In particular, the larger amount of defects necessary when an unrelaxed lattice is assumed is due to the absence of strain, while the difference between the cases of relaxation performed with the TS and SW potentials is due to the larger amount of strain generated by the latter. The largest overestimate given by the random defect model is due not only to the lack of

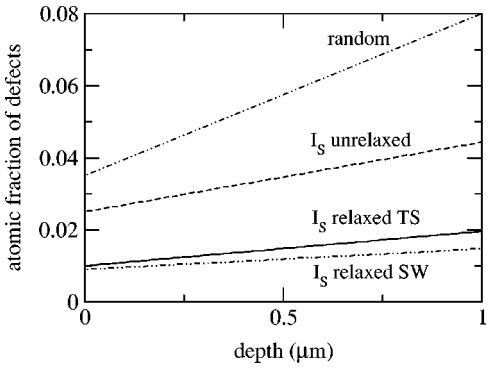

FIG. 5. Concentration of split interstitials plus vacancies versus depth (expressed as the fraction of the total number of atoms) that reproduces the experimental spectrum in the depth interval [0–1] μm, along the ⟨100⟩ alignment, according to three different damage models: unrelaxed defects, defects relaxed with the TS potential, and defects relaxed with the SW potential. For comparison, the profile obtained from the standard random defect model (''random'' curve) is reported too.

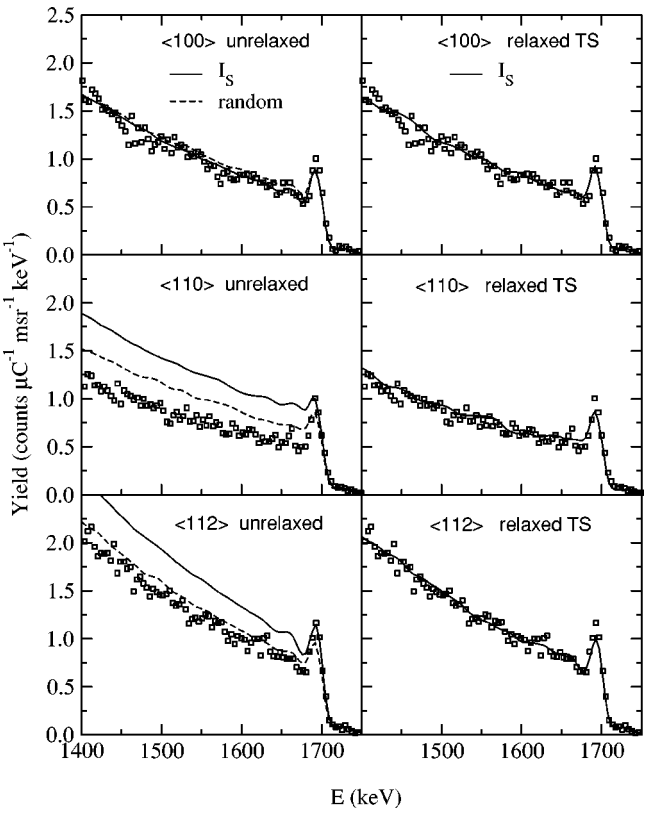

FIG. 6. Results of the multiaxial fit of experimental RBS-C spectra performed with different damage models, using the distribution of I_S plus vacancies or of the randomly displaced atoms, which reproduces the $\langle 100 \rangle$ spectrum (see Fig. 5). Symbols refer to the experimental spectra, lines refer to simulations.

relaxation, but also to the procedure followed for positioning disordered atoms. In fact, their displacement from lattice sites, chosen according to a random distribution, is, on average, lower than the one characteristic of the open-volume-symmetrical interstitial sites. For this reason they are expected to give a smaller contribution to the increase of backscattering yield than unrelaxed I_S defects.

We have thereafter tried to fit RBS-C spectra in the $\langle 110 \rangle$ and $\langle 112 \rangle$ axes with the profiles of Fig. 5. The comparison of experimental and simulated spectra under the three alignment conditions is reported in Fig. 6 for the two cases of unrelaxed defects (both I_s and random), and defects relaxed with the TS potential. While a very good multiaxial fitting is obtained using the relaxed supercell, unrelaxed I_S or random defects fail to simultaneously reproduce the spectra under all alignment conditions. Moreover, we have verified that any possible combination of unrelaxed defects is unable to fit all experimental spectra as well. On the other side, supercells containing I_S defects and relaxed with the SW potential give a good multiaxial fitting too, although in this case the estimate of defect concentration is lower (Fig. 5). The other remarkable result is that the same multiaxial fit was not possible if using I_T and I_H defects relaxed with either the TS or SW potential. We have verified that in all cases, the uncertainties in the calculated spectra due to the uncertainties in the energy loss of channeled He ions,[37] are very small and do not affect the fitting of experiments.

We can summarize the above results as follows:

(i) There is no simple combination of unrelaxed defects capable of simultaneously reproducing RBS-C spectra along different axes;

(ii) Using relaxed defects, a multiaxial fit is possible, and the amount of required damage depends on the potential (TS/EDIP or SW) used to relax the supercell;

(ii) The result is sensitive to the nature of the defect: in our case the only relaxed interstitial configuration which gives a good multiaxial fit of RBS-C spectra is the I_S one.

Despite the simplicity of the model system used here, these results show that the improvement in microscopic modeling of point defects has led to an improvement in the capability of RBS-C to interpret implantation damage in Si.

IV. CONCLUSIONS

In the present work we have reported the modeling of RBS-C response from a disordered Si lattice in which the atomic rearrangement (relaxation) originated by the insertion of a low concentration of simple point defects is modeled by the application of empirical potentials. The results reported here, beside their impact on the basic treatment of ion dechanneling due to point defects, are expected to have practical consequences in the qualitative and quantitative interpretation of RBS-C spectra of irradiated crystals. First of all, we have shown that lattice relaxation which follows the insertion of point defects increases the disorder, giving appreciable contribution to ion dechanneling. If relaxation effects are neglected (as in the standard damage models used so far), a higher amount of defects in general must be assumed to interpret RBS-C spectra. The enhancement in RBS-C yield has been shown to be dependent on the empirical potential used to relax defects, on the type of defect, and on beam-sample alignment. While the TS and EDIP potentials give results which are equivalent within the statistical errors of the simulations, the yield enhancement given by the SW potential is in general larger than the one given by the other two. It is noteworthy that this result differs from that found in the simulation of DXS patterns, which have been shown to be insensitive to the potential used to relax point defects.[26] The anisotropy in yield enhancement due to relaxation may prevent a multiaxial fitting of RBS-C experiments with a single distribution of unrelaxed defects. Preliminary results obtained in the near-surface region of samples implanted with MeV ions have confirmed this hypothesis. In fact, a good simultaneous fit of the $\langle 100 \rangle$, $\langle 110 \rangle$, and $\langle 112 \rangle$ RBS-C spectra has been obtained only when using relaxed defects. Moreover, it has been found that only a supercell populated with relaxed split-$\langle 110 \rangle$ self interstitials may reproduce the experiments.

Radiation damage in ion-implanted Si is expected to be more complex than the model system considered here. Nevertheless, we have demonstrated that a description of disorder based on a more accurate model of simple point defects may give a consistent interpretation of multiaxial RBS-C

analysis of an ion-implanted layer containing a low level of disorder. The extension of the method to higher concentrations and more complex configurations of defects will be the matter of future investigation.

ACKNOWLEDGMENTS

The authors wish to thank A. M. Mazzone for helpful discussions and R. Lotti for technical assistance.

*Electronic address: lulli@lamel.bo.cnr.it

[1] F. H. Stillinger and T. A. Weber, Phys. Rev. B **31**, 5262 (1985).
[2] J. Tersoff, Phys. Rev. B **38**, 9902 (1988).
[3] J. F. Justo, M. Z. Bazant, E. Kaxiras, V. V. Bulatov, and S. Yip, Phys. Rev. B **58**, 2539 (1998).
[4] T. Diaz de la Rubia and G. H. Gilmer, Phys. Rev. Lett. **74**, 2507 (1995).
[5] M. J. Caturla, T. Diaz de la Rubia, L. A. Marques, and G. H. Gilmer, Phys. Rev. B **54**, 16 683 (1996).
[6] K. Nordlund and R. S. Averback, Phys. Rev. B **56**, 2421 (1997).
[7] K. Nordlund, M. Ghaly, R. S. Averback, M. Caturla, T. Diaz de la Rubia, and J. Tarus, Phys. Rev. B **57**, 7556 (1998).
[8] W. Windl, T. J. Lenosky, J. D. Kress, and A. F. Voter, Nucl. Instrum. Methods Phys. Res. B **141**, 61 (1998).
[9] M. Mazzarolo, L. Colombo, G. Lulli, and E. Albertazzi, Phys. Rev. B **63**, 195207 (2001).
[10] C. Z. Wang, C. T. Chan, and K. M. Ho, Phys. Rev. Lett. **66**, 189 (1991).
[11] D. J. Chadi, Phys. Rev. B **46**, 9400 (1992).
[12] E. G. Song, E. Kim, Y. H. Lee, and Y. G. Hwang, Phys. Rev. B **48**, 1486 (1993).
[13] S. J. Clark and G. J. Ackland, Phys. Rev. B **56**, 47 (1997).
[14] M. Tang, L. Colombo, J. Zhu, and T. Diaz de la Rubia, Phys. Rev. B **55**, 14 279 (1997).
[15] N. Bernstein and E. Kaxiras, Phys. Rev. B **56**, 10 488 (1997).
[16] M. J. Puska, S. Pöykkö, M. Pesola, and R. M. Nieminen, Phys. Rev. B **58**, 1318 (1998).
[17] A. Antonelli, E. Kaxiras, and D. J. Chadi, Phys. Rev. Lett. **81**, 2088 (1998).
[18] F. Cargnoni, C. Gatti, and L. Colombo, Phys. Rev. B **57**, 170 (1998).
[19] W.-K. Leung, R. J. Needs, G. Rajagopal, S. Itoh, and S. Ihara, Phys. Rev. Lett. **83**, 2351 (1999).
[20] Y. H. Lee, N. Gerasimenko, and J. Corbett, Phys. Rev. B **14**, 4506 (1976).
[21] B. C. Larson, J. Appl. Phys. **45**, 2 (1974).
[22] E. Bøgh, Can. J. Phys. **46**, 653 (1968).
[23] G. Bai and M.-A. Nicolet, J. Appl. Phys. **70**, 3551 (1991).
[24] R. Nipoti, M. Servidori, M. Bianconi, and S. Milita, Nucl. Instrum. Methods Phys. Res. B **120**, 64 (1996).
[25] P. J. Partyka, R. S. Averback, K. Nordlund, I. K. Robinson, D. Walko, P. Erhart, T. Diaz de la Rubia, and M. Tang, Mater. Res. Soc. Symp. Proc. **438**, 77 (1997).
[26] K. Nordlund, U. Beck, T. H. Metger, and J. R. Patel, Appl. Phys. Lett. **76**, 846 (2000).
[27] K. Nordlund, P. Partyka, R. S. Averback, I. K. Robinson, and P. Erhart, J. Appl. Phys. **88**, 2278 (2000).
[28] L. C. Feldman, J. M. Mayer, and S. T. Picraux, *Material Analysis by Ion Channeling* (Academic Press, New York, 1982).
[29] K. Gärtner, K. Hehl, and G. Schlotzhauer, Nucl. Instrum. Methods Phys. Res. B **4**, 55 (1984).
[30] J. Lindhard, Mat. Phys. Medd. K. Dan. Vidensk Selsk.**34**, no. 14 (1965).
[31] J. H. Barrett, Phys. Rev. B **3**, 1527 (1971).
[32] P. J. M. Smulders and D. O. Boerma, Nucl. Instrum. Methods Phys. Res. B **29**, 471 (1987).
[33] B. Weber, E. Wendler, K. Gärtner, D. M. Stock, and W. Wesch, Nucl. Instrum. Methods Phys. Res. B **118**, 118 (1996).
[34] E. Albertazzi, M. Bianconi, G. Lulli, R. Nipoti, and M. Cantiano, Nucl. Instrum. Methods Phys. Res. B **118**, 128 (1996).
[35] E. Albertazzi, M. Bianconi, G. Lulli, R. Nipoti, A. Carnera, and C. Cellini, Nucl. Instrum. Methods Phys. Res. B **112**, 152 (1996).
[36] G. Lulli, M. Bianconi, A. Parisini, S. Sama, and M. Servidori, J. Appl. Phys. **88**, 3993 (2000).
[37] G. Lulli, E. Albertazzi, M. Bianconi, G. G. Bentini, and R. Lotti, Nucl. Instrum. Methods Phys. Res. B **170**, 1 (2000).
[38] M. T. Robinson and I. M. Torrens, Phys. Rev. B **9**, 5008 (1974).
[39] G. Hobler, Nucl. Instrum. Methods Phys. Res. B **96**, 155 (1995).
[40] G. Lulli, E. Albertazzi, M. Bianconi, and R. Nipoti, Nucl. Instrum. Methods Phys. Res. B **148**, 573 (1999).
[41] S. Balboni, Ph.D. thesis, University of Bologna, Bologna, Italy (2002).
[42] M. Nastar, V. V. Bulatov, and S. Yip, Phys. Rev. B **53**, 13 521 (1996).
[43] C. Flensburg and R. F. Stewart, Phys. Rev. B **60**, 284 (1999).
[44] W. D. Luedtke and U. Landman, Phys. Rev. B **40**, 1164 (1989).